Improving the Photocatalytic Performance of Mesoporous Titania Films by Modification with Gold Nanostructures

Inga Bannat,[†] Katrin Wessels,[†] Torsten Oekermann,[†] Jiri Rathousky,[‡] Detlef Bahnemann,[§] and Michael Wark*,[†]

Institutes of Physical Chemistry and Electrochemistry and of Technical Chemistry, Leibniz Universität Hannover, Callinstrasse 3A and 5, D-30167 Hannover, Germany, and J. Heyrovsky Institute of Physical Chemistry, v.v.i., Academy of Sciences of the Czech Republic, Dolejskova 3, CZ-18223 Prague 8, Czech Republic

Received December 22, 2008

This work focuses on the synthesis and photocatalytic performance of mesoporous TiO_2 films containing embedded gold nanostructures. The TiO_2 films were prepared by the EISA (evaporation-induced self-assembly) process and loaded with Au either by impregnation followed by reduction with $NaBH_4$ or by pulsed cathodic electrodeposition. The latter approach represents a considerably easier and faster synthetic method and results in dendritic Au nanostructures as a replica of the pore system. The as-prepared composite films were characterized by scanning and transmission electron microscopy (SEM and TEM), UV−vis spectroscopy and Kr adsorption. Photocatalytic oxidation of NO was chosen as the test reaction for elimination of air pollutants. For mesoporous TiO_2 films deposited on an ITO layer, the photonic efficiency is higher than for films prepared on glass, because the pore structures are altered. Incorporation of Au results in a significant improvement in the photonic efficiency due to the generation of Schottky barriers, which inhibit the recombination of electron−hole pairs and thereby increase the concentration of photogenerated holes at the film surface reacting with NO. Compared to the impregnated nanocomposites, mesoporous TiO_2 films with electrochemically incorporated dendritic Au nanostructures provide comparable photocatalytic activities, but their preparation is much less time-consuming and of lower cost. An additional treatment with O_2 plasma leads to further increase in the photocatalytic activity due to the higher amount of hydroxyl groups on the surface, which play a significant role in the photocatalytic oxidation of NO. Mesoporous nanocomposite films are promising in photocatalysis and self-cleaning technologies.

I. Introduction

Titanium dioxide is one of the most important semiconductors, with applications in solar cells,[1] photocatalysis,[2] and catalyst support.[3] Its performance is often enhanced by the incorporation of particles of noble metals like Pt, Ag, or Au.[4−6] Gold nanoparticles in particular have recently attracted much attention because of their interesting catalytic and optical properties.[7−10] Gold and silver nanoparticles absorb light in the visible range due to surface plasmon resonance, which is a light-induced collective oscillation of conducting electrons on the surface of a metal. This phenomenon strongly depends on the particle size and shape and the dielectric environment, leading for gold nanoparticles to a wide and diverse color spectrum[11−13] and making them most interesting for use in biosensors and nanodevices.[14,15]

Mesoporous thin films of TiO_2 are among the best candidates as a host matrix for embedding metal nanoparticles and nanostructured metal arrays because of their tunable and well-defined pore systems. Generally, ordered mesoporous films of metal oxides, such as silicon, titanium, zirconium, and tungsten oxides, with a large surface area, controlled and well-defined pore ordering, and amorphous or nanocrystalline pore walls can be easily obtained by a generalized sol−gel procedure based on a mechanism that combines evaporation-induced self-assembly of a block

* To whom correspondence should be addressed: e-mail Michael.Wark@pci.uni-hannover.de.
[†] Institute of Physical Chemistry and Electrochemistry, Leibniz Universität Hannover.
[‡] Academy of Sciences of the Czech Republic.
[§] Institute of Technical Chemistry, Leibniz Universität Hannover.

(1) O'Reagan, B.; Grätzel, M. *Nature* **1991**, *353*, 737.
(2) Tschirch, J.; Bahnemann, D.; Wark, M.; Rathousky, J. *J. Photochem. Photobiol., A* **2008**, *194*, 181.
(3) Milsom, E. V.; Perrott, H. R.; Peter, L. M.; Marken, F. *Langmuir* **2005**, *21*, 6341.
(4) Keller, V.; Bernhardt, P.; Garin, F. *J. Catal.* **2002**, *215*, 129.
(5) Sclafani, A.; Mozzanega, M.-N.; Pichat, P. *J. Photochem. Photobiol., A* **1991**, *59*, 181.
(6) Li, H.; Bian, Z.; Zhu, J.; Huo, Y.; Li, H.; Lu, Y. *J. Am. Chem. Soc.* **2007**, *129*, 4538.
(7) Templeton, A. C.; Pietron, J.; Murray, R.; Mulvaney, P. *J. Phys. Chem. B* **2000**, *104*, 564.
(8) Aldous, L.; Silvester, D. S.; Villagran, C.; Pitner, W. R.; Compton, R. G.; Lagunas, M. C.; Hardacre, C. *New J. Chem.* **2006**, *30*, 1576.
(9) Li, X. B.; Wang, H. Y.; Yang, X. D.; Zhu, Z. H.; Tang, Y. J. *J. Chem. Phys.* **2007**, *8*, 126.
(10) Yu, K.; Tian, Y.; Tatsuma, T. *Phys. Chem. Chem. Phys.* **2006**, *8*, 5417.
(11) Faraday, M. *Philos. Trans.* **1857**, *147*, 145.
(12) Mie, G. *Ann. Phys.* **1908**, *330*, 377.
(13) Kelly, K. L.; Coronado, E.; Zhao, L. L.; Schatz, G. C. *J. Phys. Chem. B* **2003**, *107*, 668.
(14) Dubertret, B.; Calame, M.; Libchaber, A. J. *Nat. Biotechnol.* **2001**, *19*, 365.
(15) Andres, R. P.; Bein, T.; Dorogi, M.; Feng, S.; Henderson, J. I.; Kubiak, C. P.; Mahoney, W.; Osifchin, R. G.; Reifenberger, R. *Science* **1999**, *272*, 1323.

10.1021/cm803455k CCC: $40.75
Published on Web 03/20/2009

copolymer with complexation of molecular inorganic species.[16−18] To fabricate gold metal nanostructures within these well-arranged pore systems consisting of SiO_2, several procedures have been published. Yang et al.[19] reported the synthesis of gold nanowire networks in mesoporous silica by using positively charged functional groups on the pore surface, which serve as capping agent for the $AuCl_4^-$ ions and facilitate the formation of nanowires. Other synthesis procedures, such as chemical reduction of the noble metal precursors, deposition−precipitation method, or electrodeposition of metal wires within anodized aluminum oxide membranes as templates, have also been successfully applied,[20−22] providing metal nanowires or nanoparticle arrays embedded within an insulating matrix. In contrast, TiO_2 serving as substrates for the incorporation of gold nanostructures offer tunable properties due to the metal−semiconductor interactions. However, only a few studies were reported on the use of ordered mesoporous TiO_2 films as templates for the formation of gold nanoparticle arrays or nanowires and the photocatalytic performance of the resulting composites. Li et al.[6] synthesized mesoporous Au/TiO_2 nanocomposites by a multicomponent assembly approach, where surfactant, titania, and gold building clusters were cooperatively assembled in a one-step process. In their study, the gold nanoparticles embedded within the mesoporous matrix led to an enhancement of the photocatalytic activity in chromium reduction and phenol oxidation depending on the loading with Au. An incorporation of gold nanoparticle arrays within the ordered mesopores of a TiO_2 film by electrodeposition was first tried by Perez et al.[23] The mesoporous film was immersed in deposition solution containing $HAuCl_4$ for 10 h, allowing the diffusion of gold ions into the pores. By starting the deposition at 0.80 V versus standard calomel electrode (SCE) and decreasing it stepwise to 0.65 V versus SCE, red-bluish mesoporous Au/TiO_2 films were obtained after 120 min. However, an inhomogeneous gold film was formed on the external surface of the mesoporous films, indicating the growth of gold outside the pores, which leads to their blocking. Nevertheless, electrodeposition techniques have many advantages such as low cost and the possibility to scale up the method for application to large areas. Pulsed electrodeposition, utilizing short high-potential pulses to nucleate particle growth at a much higher number of sites than the lower voltage continuous deposition, was applied to deposit metal particles, for example, gold nanoparticles with diameters of 5−150 nm, on thin anatase films with random pore ordering supported on titanium foils, on metal alloys, and on nanoparticulate metal oxide films, improving in all cases the mechanical and physical properties.[24−26]

For our studies, we used mesoporous TiO_2 films with defined mesoporosity, that is, narrow pore size distributions, synthesized via sol−gel technique according to the EISA process, as the template matrices. Two different methods were used for the incorporation of gold nanostructures: (1) modification of the TiO_2 surface with capping agents, followed by impregnation with Au(III) ions and their reduction with $NaBH_4$; and (2) pulsed potentiostatic electrodeposition from $HAuCl_4/HClO_4$ solution. The following questions were addressed: (i) Which morphologies of the incorporated Au nanostructures can be obtained by using the impregnation method and pulsed electrodeposition? (ii) Are there advantages of the pulsed electrodeposition method compared to the impregnation method? (iii) Is there an influence of the incorporated gold on the photocatalysis depending on the approach used?

II. Experimental Section

Indium tin oxide-coated glass sheets (ITO, Visiontek Systems Ltd.) with a resistance of 13−18 Ω/square, served as conducting substrates for the deposition of mesoporous films. Titanium(IV) ethoxide (Merck), titanium(IV) chloride (99.9%, Acros), ethanol (99.8%, Roth), hydrochloric acid (37 wt %, p.a., Riedel-de Haen), hydrogen tetrachloroaurate(III) hydrate ($HAuCl_4 \cdot H_2O$, 99.9%, Chempur), potassium hydroxide (97%, Acros), sodium borohydride (95%, Riedel-de Haen), anhydrous methylene dichloride (99.8%, Aldrich), 3-mercaptopropyl trimethoxysilane (3-MPTMS, >95%, Merck), and perchloric acid ($HClO_4$, p.a., Acros) were used as received without further purification. The block copolymer Pluronic P 123 ($EO_{20}PO_{70}EO_{20}$) was purchased from BASF. Solutions for electrochemistry were prepared in deionized water with a resistivity of about 18 MΩ·cm.

Sample Preparation. Thin mesoporous TiO_2 films with wormlike structure were prepared according to the procedure given elsewhere.[18] Titanium(IV) ethoxide (33.6 g) was dissolved in 21.6 mL of concentrated HCl (37 wt %) under vigorous stirring. After 5 min, a solution of 8.0 g of Pluronic P 123 in 96.0 g of ethanol was added. The resulting solution was used for dip-coating ITO-coated glass or microscope glass slides at a constant withdrawal rate of 80 mm min^{-1} at 20 °C and a relative humidity of 15%. The films were aged for at least 5 h and calcined in air at 400 °C for 4 h (heating rate 1 °C min^{-1}).

The surface of mesoporous TiO_2 films was functionalized with thiol groups using a 10 mmol L^{-1} solution of 3-MPTMS in methylene dichloride, followed by repeated washing with methylene dichloride and ethanol according to the procedure given elsewhere.[27] Afterward the films were soaked with a solution prepared by mixing 0.5 mL of a 5.0 M KOH solution and 1 mL of a 0.5 M aqueous $HAuCl_4$. Different gold loadings were obtained by varying the impregnation time from 5 to 180 min. Subsequently, the Au(III) ions were reduced by 10 mL of a 0.1 M $NaBH_4$ aqueous solution.

Alternatively, gold was electrodeposited cathodically from an Ar-saturated aqueous solution containing 70 μM $HAuCl_4$ and 10

(16) Brinker, C. J.; Lu, J.; Sellinger, A.; Fan, H. *Adv. Mater.* **1991**, *11*, 579.
(17) Alberius, P. C. A.; Frindell, K. L.; Hayward, R. C.; Kramer, E. J.; Stucky, G. D.; Chmelka, B. F. *Chem. Mater.* **2002**, *14*, 3284.
(18) Wark, M.; Tschirch, J.; Bartels, O.; Bahnemann, D.; Rathousky, J. *Microporous Mesoporous Mater.* **2005**, *84*, 247.
(19) Yang, C. M.; Sheu, H. S.; Chao, K. J. *Adv. Funct. Mater.* **2002**, *12*, 143.
(20) Han, Y. J.; Kim, J. M.; Stucky, G. D. *Chem. Mater.* **2000**, *12*, 2068.
(21) Zanella, R.; Giorgio, S.; Shin, C.-H.; Henry, C. R. *J. Catal.* **2004**, *222*, 357.
(22) Sauer, G.; Brehm, G.; Schneider, S.; Nielsch, K.; Wehrspohn, R. B.; Choi, J.; Hofmeister, H.; Gösele, U. J. *Appl. Phys.* **2002**, *91*, 3243.
(23) Perez, M. D.; Otal, E.; Bilmes, S. A.; Soler-Illia, G. J. A. A.; Crepaldi, E. L.; Grosso, D.; Sanchez, C. *Langmuir* **2004**, *20*, 6879.
(24) Beack, S. H.; Jaramillo, T. F.; Stucky, G. D.; McFarland, E. W. *Nano Lett.* **2002**, *2*, 831.
(25) Tang, J.; White, M.; Stucky, G. D.; McFarland, E. W. *Electrochem. Commun.* **2003**, *5*, 497.
(26) Baeck, S.-H.; Jaramillo, T. F.; Kleiman-Shwarsctein, A.; McFarland, E. W. *Meas. Sci. Technol.* **2005**, *16*, 54.
(27) Marschall, R.; Bannat, I.; Caro, J.; Wark, M. *Microporous Mesoporous Mater.* **2007**, *99*, 190.

mM $HClO_4$ in a three-electrode electrochemical cell with a Pt counter electrode and an Ag/AgCl reference electrode (−0.045 V versus SCE). The mesoporous TiO_2 films on ITO-coated glass served as a working electrode. For pulsed electrodeposition, rectangular potential pulses were used. During each pulse, a potential of −6.0, −3.0, or −1.0 V versus Ag/AgCl was applied for 3 s, followed by a potential of +0.1 V versus Ag/AgCl being applied for 1 s. The number of consecutive pulses was varied between 1 and 32. The obtained films were rinsed with water and dried in air.

Experimental Methods. A potentiostat/galvanostat (Autolab 12, Eco Chemie) with GPES software for the collection and analysis of data was used for pulsed electrodeposition.

Scanning electron microscopy (SEM) micrographs were obtained from a Jeol JSM-6700F field-emission instrument with the secondary electron detector at a low acceleration voltage of 5 kV. Transmission electron microscopy (TEM) was performed on a Jeol JEM-2100F field-emission instrument at 200 kV with an ultra-high-resolution pole piece and a spherical aberration constant of CS = 0.5 mm that provides a point resolution better than 0.19 nm. Moreover, the microscope was equipped with a Gatan GIF 2001 energy filter with a 1k-CCD (charge-coupled device) camera. Specimens for the TEM investigation were prepared by epoxy agglutination of two film pieces. Subsequently, these samples were first cut into $1 \times 1 \times 2$ mm^3 pieces, ground, and polished on polymer-embedded diamond lapping films to approximately 0.01 $\times 1 \times 2$ mm^3. Finally, Ar^+ ion sputtering was employed at 3 kV under an incident angle of 4° until electron transparency was achieved.

The film thickness was determined by use of a Dektak 6 M stylus (Veeco) surface profile measuring system in combination with TEM measurements.

Texture properties of the mesoporous films were determined from Kr adsorption isotherms carried out at 77 K on a Micromeritics ASAP 2010 apparatus. Prior to the adsorption experiments, the samples were outgassed at 150 °C overnight. The pore size of a mesoporous film was calculated from a correlation between pore size and point of inflection of the desorption branch of the corresponding adsorption/desorption isotherm. This correlation was obtained for a series of well-defined mesoporous films, whose porosity was studied both by krypton adsorption and by environmental ellipsometric porosimetry, demonstrating reasonable agreement for the data obtained by both techniques.[28] For estimation of texture parameters of the films from Kr isotherms, the molecular cross-sectional area of krypton of 0.21 nm^2 and the molar volume of solid krypton were used according to the software of the adsorption apparatus producer.

Photocatalytic oxidation of NO was carried out in an experimental setup consisting of a gas supply, the photoreactor, and a chemiluminescent NO−NO_x analyzer (Horiba ambient monitor APNA-360). To obtain the starting concentration of NO of 100 ppb at a relative humidity of 50%, a gaseous mixture of dry air (1500 mL min^{-1}), wet air (1500 mL min^{-1}, relative humidity 100%), and 50 ppm NO in N_2 (6 mL min^{-1}) was prepared. This gas stream was continuously flowed through the photoreactor, and photocatalytic oxidation of NO was obtained over Au/TiO_2 films with a geometric area of 15.5 cm^2 and UV light with an intensity of 1 mW cm^{-2} and mean wavelength of $\lambda = 350$ nm.

Activation of the Au/TiO_2 film surface with oxygen plasma was carried out for 5 min in a Diener Femto Qls plasma system (generator: 40 kHz/100 W) with an oxygen flow rate of 63 mL min^{-1} and a generator output of 50%.

(28) Rathousky, J.; Kalousek, V.; Walsh, C. Unpublished data, 2008.

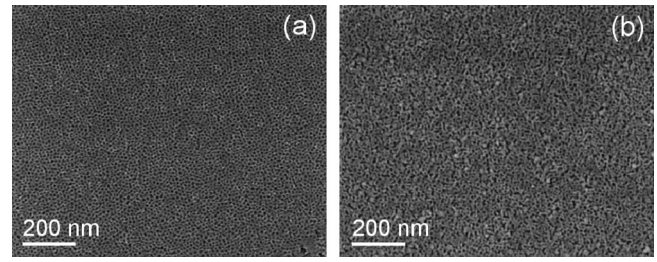

Figure 1. SEM (top view) micrographs of mesoporous TiO_2 films deposited on (a) ITO-coated substrate and (b) microscope glass slides.

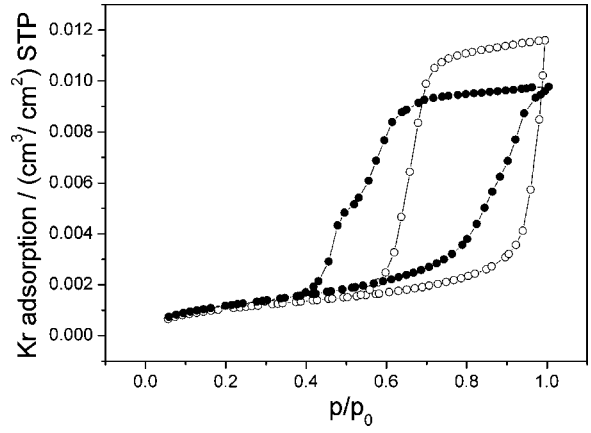

Figure 2. Sorption isotherms of Kr at 77 K on pristine mesoporous titania films on (○) microscope glass slides and (●) ITO-coated glass.

III. Results and Discussion

Mesoporous TiO_2 Films. The obtained mesoporous TiO_2 films on ITO-coated glass and microscope glass slides were optically transparent and crack-free. The thickness of the films was measured by profilometry as about 250 and 300 nm, respectively. SEM micrographs of the as-prepared TiO_2 films indicate that the substrate substantially influences the ordering of the mesopore arrangement (Figure 1). While films deposited on ITO-coated glass show a homogeneous well-ordered mesoporous structure with pores about 7−8 nm in diameter (Figure 1a), films on microscope glass slides possess a less ordered porous structure with a much broader pore size distribution and some larger pores with diameters >8 nm (Figure 1b). The difference probably arises from different affinities of the templating molecules to the substrates. Comparable results were reported previously by Chougnet et al.,[29] who studied the dependence of ordering of mesoporous SiO_2 films on the nature of the substrate. They suggested that stronger interaction of the block copolymer with the substrate leads to acceleration of the formation of ordered structure, so that the liquid crystalline phase leading to the final mesostructure is developed before condensation of the inorganic walls occurs.

Adsorption isotherms of Kr at 77 K measured for both films are of type IV, characterized by a broad hysteresis loop, which proves their highly developed mesoporosity (Figure 2). In comparison to films prepared on microscope glass slides, those deposited on ITO-coated glass substantially differ in their character of porosity; namely, their porous

(29) Chougnet, A.; Heitz, C.; Søndergard, E.; Albouy, P.-A.; Klotz, M. *Thin Solid Films* **2006**, *495*, 44.

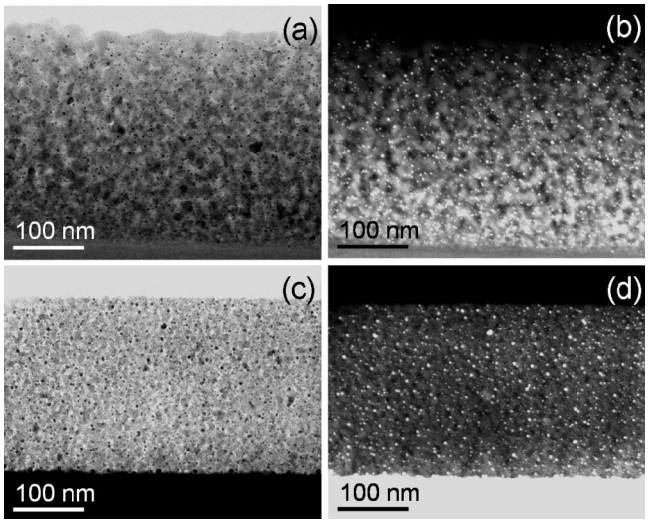

Figure 3. TEM micrographs of the cross-sectional view of thiol-modified mesoporous titania films loaded with Au nanoparticles by using an impregnation time of 5 min: (a, c) bright-field and (b, d) dark-field images of films deposited on (a, b) microscope glass slides and (c, d) ITO-coated glass.

system exhibits a bimodal pore size distribution. This follows from the shape of the adsorption isotherms, as both adsorption and especially desorption branches exhibit two regions of steep increase and decrease in amount of adsorbed Kr. This type of porosity confirms the stronger adsorption on the crystalline ITO layer. The film exhibits a specific surface area of 69 cm^2/cm^2 and specific pore volume of 0.014 mm^3/cm^2 related to the geometric area of the support. The pore sizes of ca. 7 and 8.4 nm correspond well with the value of 7−8 nm estimated from the SEM micrographs (Figure 1). In comparison, the mesoporous TiO_2 films deposited on microscope glass slides have a slightly lower specific surface area of 51 cm^2/cm^2 but a comparable specific pore volume of 0.015 mm^3/cm^2, the mean pore size being about 10 nm. The location of the lower closure points at a relative pressure of 0.4 for the film on ITO-coated glass might indicate some slight pore blocking, which is completely absent for the film on microscope glass slides, showing a closure point at a higher relative pressure of almost 0.6.

Incorporation of Au Nanoparticles by Impregnation. SEM and Kr adsorption clearly prove that the films are mesoporous with large surface area and regularly ordered mesopores. In order to incorporate the Au nanostructures within the pores by impregnation, the surface was first modified with 3-MPTMS to anchor thiol groups as capping agents within the mesopores, which leads to homogeneous distribution of gold nanoparticles. Synthesis and characterization were carried out according to a detailed study on modification of metal oxide surfaces with 3-MPTMS and their analysis by Fourier transform infrared (FT-IR) spectroscopy, which we reported previously.[27]

After the impregnation time of typically 5 min and subsequent reduction with $NaBH_4$, the transparent and crack-free films became light red, indicating the formation of Au nanoparticles. Figure 3 shows bright- and dark-field TEM micrographs of the cross-sectional area of the thiol-modified titania films after gold loading, deposited on microscope glass

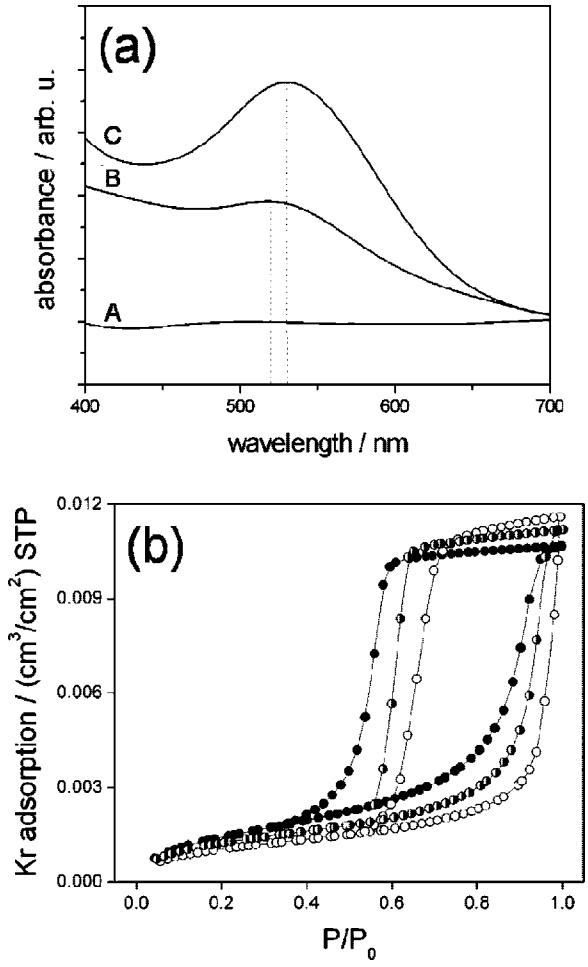

Figure 4. (a) UV−vis absorption spectra of a pristine mesoporous TiO_2 film (curve A) and of mesoporous Au/TiO_2 films on ITO-coated glass (curve B) and microscope glass slides (curve C). (b) Kr adsorption isotherms of pristine mesoporous TiO_2 films (○) and of mesoporous Au/TiO_2 films impregnated for 5 min (◑) and 3 h (●) on microscope glass slides.

slides (panels a and b) and on ITO-coated glass (panels c and d). In accordance with the investigations by SEM (Figure 1), the pore structure of the film on ITO-coated glass shows considerably smoother ordering (Figure 3c,d). In addition to the pore structure of the titania films, dark spots in the bright-field images and corresponding white spots in the dark-field images are observed, indicating the presence of spherical Au nanoparticles with diameters considerably smaller than 5 nm. They are homogeneously distributed within the whole film owing to the thiol groups, which serve as anchors for the $AuCl_4^-$ ions, reducing their mobility and, thus, controlling the location and limiting the growth of Au nanoparticles. An increase in impregnation time from 5 up to 180 min leads to higher loadings and an increase of the particle diameters up to 8−10 nm, further growth being inhibited due to the restriction by the given pore sizes of the mesoporous films. Measurements of the films on both substrates by energy-dispersive X-ray spectrometry (EDXS) gave Au:Ti ratios of about 0.08, 0.26, and 0.54 for impregnation times of 5, 20, and 180 min, respectively.

The TiO_2 and Au/TiO_2 nanocomposite films were characterized by UV−vis absorption spectroscopy as shown in Figure 4a. In contrast to the flat absorption spectrum of the pristine TiO_2 film (curve A), peaks centered at 531 and 520

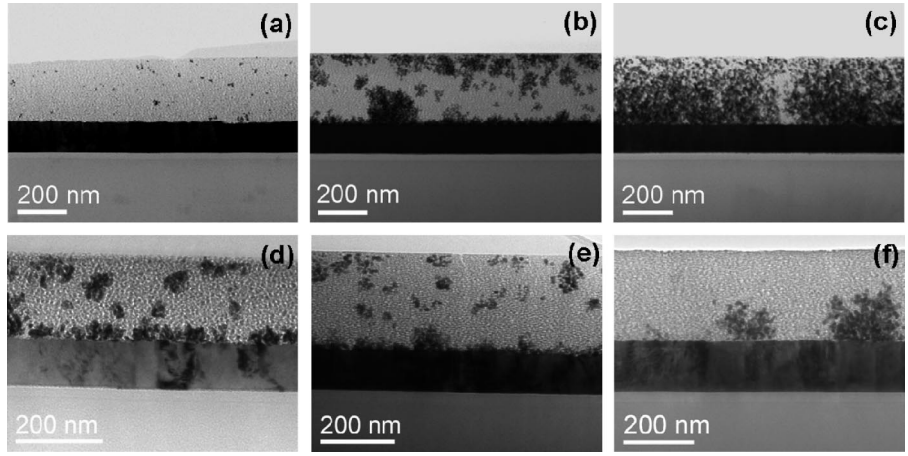

Figure 5. TEM micrographs of the cross-section of ordered mesoporous TiO_2 films on ITO-coated glass after pulsed electrodeposition of Au by application of (a) one, (b) eight, and (c) 32 pulses of −6.0 V/0.1 V. The micrographs at the bottom shows the films after application of eight pulses of (d) −6.0 V/0.1 V, (e) −3.0 V/0.1 V, and (f) −1.0 V/0.1 V.

nm were observed for the Au-loaded films on microscope glass slides (curve C) and ITO-coated glass (curve B), respectively. They correspond to the transverse surface plasmon band of spherical Au nanoparticles.[10,13] For example, Murphy et al.[30] reported an absorption band located at around 520 nm for spherical gold nanoparticles with a diameter of about 4 nm stabilized with sodium citrate in water. The comparable wavelengths of the surface plasmon resonance band indicate that there is no further influence of the refractive index and of the dielectric constant of the applied transparent thin TiO_2 film on the position, which generally leads to a red shift depending on the thickness of the film, as reported by Manera et al.[31] The similar position of plasmon bands of the nanocomposite films on ITO-coated glass and microscope glass slides confirms the formation of Au nanoparticles with equal particle sizes, which was already supposed from TEM results. The optical band gap of TiO_2 can be evaluated by the equation $\alpha = A(h\nu - E_g)^n/h\nu$, where E_g is the optical band gap, α is the absorption coefficient, A is a constant, $h\nu$ is the energy of light, and $n = 2$ for TiO_2 with an indirect, allowed energy gap. If it is assumed that the absorption coefficient α is proportional to the Kubelka−Munk function $F(R)$, the band gap energy can be obtained from the plot of $[F(R)h\nu]^{1/2}$ versus $h\nu$ and extrapolation of the linear portion near the onset of absorption edge to the energy axis. The band gap energy for the mesoporous TiO_2 thin film was estimated to be 3.55 eV, which is slightly shifted to higher energy values compared to bulk TiO_2, with an energy band gap of 3.18 eV.[32] This shift might be the result of the size-dependent quantum confinement effect[33] or the porosity of the mesoporous TiO_2 film,[34] which was found in similar studies.

Figure 4b shows Kr adsorption isotherms measured for Au/TiO_2 nanocomposite films deposited on microscope glass slides with different impregnation times. The isotherms prove that the mesoporosity of the pristine films is only slightly modified by the surface modification and the introduction of gold nanoparticles. For an impregnation time of 3 h, the specific pore volume decreased from 0.015 to 0.013 mm^3/cm^2 and the pore size from 10 to 7 nm; shorter impregnation times of, for example, 5 min led to even smaller changes. The steepness of the adsorption branches as well as the desorption branches in the Kr isotherms of both loaded samples shows that the pore size distribution has remained narrow. It can be concluded that all the important characteristics of the mesoporous system are preserved in the modified films and that no general pore blocking occurred. The observed narrowing of the pore size, however, might lead to some hindering of diffusion in the pores, influencing the photocatalytic behavior (see below).

Incorporation of Dendritic Au Nanostructures by Electrochemical Deposition. In the alternative approach, Au/TiO_2 nanocomposite films were prepared by pulsed electrodeposition. In this case a conductive substrate such as ITO-coated glass is needed. This method led to the formation of dendritic Au nanostructures within the pore system (Figure 5). The applied potential pulses lead to progressive nucleation followed by controlled growth. Each pulse applied at high negative potential creates additional gold nuclei within the mesopores, followed by their further growth at slightly positive potential. The combination of nucleation and growth finally results in the generation of dendritic gold nanostructures as a replica of the wormlike pore system. The different phases obtained by pulsed electrodeposition at −6.0 V/0.1 V with one, eight, and 32 pulses are shown in Figure 5a−c. The cross-section of the film after application of one single pulse demonstrates the assumed nucleation (Figure 5a). At positive potential in the second phase of the pulse sequence, the Au nuclei grow to isolated particles with diameters of 2−10 nm. As a consequence, this film appears light red, indicating the presence of small spherical nanoparticles. The observed particles are distributed over the whole film due to the high conductivity of the TiO_2 framework induced by the applied high negative potential during the pulse. The generation of dendritic gold nanostructures can be observed

(30) Murphy, C. J.; Sau, T. K.; Gole, A. M.; Orendorff, C. J.; Gao, J.; Gou, L.; Hunyadi, S. E.; Li, T. *J. Phys. Chem. B* **2005**, *109*, 13857.
(31) Manera, M. G.; Spadavecchia, J.; Buso, D.; De Julian Fernandez, C.; Mattei, G.; Martucci, A.; Mulvaney, P.; Perez-Juste, J.; Rella, R.; Vasanelli, L.; Mazzoldi, P. *Sens. Actuators, B* **2008**, *132*, 107.
(32) Linsebigler, A. L.; Lu, G.; Yates, J. T. *Chem. Rev.* **1995**, *95*, 735.
(33) Chen, Y.; Stathatos, E.; Dionysiou, D. D. *Surf. Coat. Technol.* **2008**, *202*, 1944.
(34) Fu, Y.; Jin, Z.; Xue, W.; Ge, Z. *J. Am. Ceram. Soc.* **2008**, *91*, 2676.

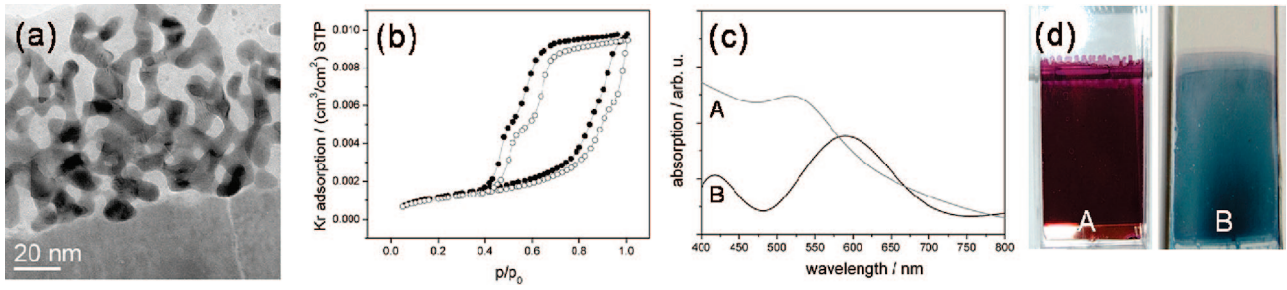

Figure 6. (a) High-resolution TEM micrograph of dendritic Au nanostructures embedded in a titania matrix. (b) Kr sorption isotherms of a pristine mesoporous titania film (○) and a titania film loaded with dendritic Au nanostructures (●). (c) UV−vis absorption spectra of mesoporous titania films with Au nanoparticles synthesized by impregnation (5 min) (spectrum A) and electrodeposited Au nanostructures (spectrum B). (d) Images of the colored films corresponding to the measurements shown in panel c. All films were deposited on ITO-coated glass, and the electrodeposition was performed with eight pulses at −6.0 V/0.1 V.

after application of additional pulses, with the resulting films appearing blue in color. This is due to the domination of larger particles with sizes determined by the width of the pore system. After eight pulses (Figure 5b), the dendritic structures are still separated from each other, leaving larger areas free of Au in the film. Almost complete filling of the pore structure could be achieved after 32 pulses (Figure 5c). Analysis of EDXS measurements revealed Au:Ti ratios of 0.01, 0.084, and 0.77 after one, eight, and 32 pulses, respectively.

To achieve growth of gold nanostructures only directly from the ITO substrate, the negative potential for the nucleation of Au particles has to be reduced. This is demonstrated in Figure 5d−f, where the negative potential of the pulses has been reduced from −6.0 V (d) to −3.0 V (e) and −1.0 V (f). As expected, Figure 5d looks similar to Figure 5b, since the same potentials and number of pulses were applied. The decrease in negative potential to −3.0 V (Figure 5e) already leads to a reduced growth of Au nanostructures deep inside the mesoporous TiO_2 film with respect to growth starting from the conducting ITO substrate. Finally, a potential of −1.0 V results in exclusive growth of the pore-filling dendritic gold nanostructures from the conductive ITO substrate.

Figure 6a shows a high-resolution TEM image of the dendritic Au nanostructures electrodeposited with eight pulses at −6.0 V/0.1 V, consisting of branched nanowires embedded in the mesoporous TiO_2 film. This structure is quite different from the chains of nanoparticles reported previously by Perez et al.,[23] which were synthesized by electrodeposition with decreasing potential ramp. The nanowires are about 8 nm in diameter, in agreement with the width of the pores, and exhibit lengths up to several hundred nanometers.

The Kr sorption isotherms of both the pristine film and that containing the electrodeposited nanostructures show that the encapsulation of Au has led to some expected decrease in both the surface area (from 69 to 53 cm^2/cm^2) and the pore volume (from 0.014 to 0.012 mm^3/cm^2), the overall character of the porosity being, however, preserved (Figure 6b).

In order to compare the light absorption properties of both types of Au/TiO_2 nanocomposites, films with identical Au:Ti ratios of about 0.08 were prepared on ITO-coated glass by both techniques, namely, by impregnation for 5 min followed by reduction, resulting in a red film, and by pulsed electrodeposition with eight pulses at −6.0 V/0.1 V, which leads to a bluish color (Figure 6d). The UV−vis absorption spectrum of the dendritic Au nanostructures shows a rather intense absorption maximum at 590 nm, while impregnation and reduction leads to a weaker absorption maximum at 520 nm (Figure 6c). In general, anisotropic gold nanorods are known to show a splitting of the surface plasmon resonance band of gold into two absorption bands. The one at shorter wavelength corresponds to absorption and scattering of light along the short transverse axis of the nanostructures, while the one at longer wavelength belongs to absorption and scattering of light along the longitudinal axis. The position of the longitudinal absorption band is influenced by the aspect ratio of rodlike nanoparticles and can be tuned from visible to near-IR by changing the aspect ratio.[30,35] In the present study, electrodeposition led to the formation of dendritic nanostructures of gold, which were formed instead of ideal anisotropic nanorods. Only a few studies on branched Au nanocrystals, so-called tripod particles, were reported.[36,37] It was found that the two plasmon bands were merged in the range of about 600−700 nm caused by in-plane excitations associated with the tips of the branched crystals, which was also confirmed by discrete dipole approximation (DDA) electrodynamics calculations. These results agree well with the absorption band at about 590 nm of the dendritic Au nanostructures synthesized by pulsed electrodeposition.

In summary, the results of pulsed electrodeposition show numerous advantages compared to the impregnation method and to electrodeposition at constantly decreasing potential reported by Perez et al.:[23] (i) Considerable time saving is achieved, since by pulsed electrodeposition a Au:Ti ratio of about 0.08 is obtained within 40 s, in contrast to 5 min of impregnation and subsequent reduction with $NaBH_4$ or 10 h of impregnation followed by applying a potential ramp for 2 h as described by Perez et al..[23] (ii) The incorporation of Au can be carried out without further steps like modification of the semiconductor surface and reduction of the metal precursor. (iii) Not only Au nanoparticles but also dendritic

(35) Jain, P. K.; Eustis, S.; El-Sayed, M. A. *J. Phys. Chem. B* **2006**, *110*, 18243.
(36) Hao, E.; Bailey, R. C.; Schatz, G. C.; Hupp, J. T.; Li, S. *Nano Lett.* **2004**, *4*, 327.
(37) Kang, S. K.; Lee, J.; Kim, Y.; Yi, J. *Curr. Appl. Phys.* **2008**, *8*, 810.

Au nanostructures representing a replica of the pore system can be formed.

Photocatalytic Properties. Mesoporous TiO_2 films loaded with either nanoparticles or dendritic nanostructures with Au:Ti ratio about 0.08 were tested in the photocatalytic oxidation of NO. As the TiO_2 used is a semiconductor with a band gap of 3.55 eV, electron−hole pairs can be generated by absorption of UV light with wavelengths under 350 nm. On the film surface the photogenerated holes react with OH^- ions or H_2O molecules, yielding highly oxidative hydroxyl ($OH^\bullet$) radicals, which are the key oxidants in the photocatalytic oxidation process.[32,38−40] These radicals quickly react with absorbed NO to HNO_2, which is further oxidized to NO_2 and H_2O. NO_2 is either desorbed or converted to HNO_3. The photogenerated electrons are consumed by adsorbed oxygen molecules.[41−43]

Photonic efficiency ξ, which is defined as the ratio of the degradation rate of NO and the incident photon flux related to the illuminated area, was calculated according to

$$\xi = \frac{hcN_A\Delta\dot{n}_{NO}}{\Phi A\lambda}$$

where h is Planck's constant, c is light velocity, N_A is Avogadro's constant, $\Delta\dot{n}_{NO}$ is the difference between inlet and outlet flux of NO, Φ is light intensity, A is illuminated area, and λ is the wavelength of UV light. Complete degradation of NO with an initial concentration of 100 ppb, which corresponds to $\Delta\dot{n}_{NO} = 2.1 \times 10^{-10}$ mol s^{-1}, results in a maximum theoretical photonic efficiency ξ_{th} of 0.45%. All efficiencies of the analyzed samples were calculated after 90 min testing time to ensure steady-state behavior and to avoid adsorption/desorption effects typically occurring in the beginning of the measurement. To compare the results of the different tested samples, the photocatalytic activity was defined as the ratio of measured photonic efficiency ξ to theoretical photonic efficiency ξ_{th}.

Figure 7 shows the activities of pristine and gold-loaded TiO_2 films in comparison to commercial Sto Photosan Color as reference. Photosan, offered by the company Sto, contains a photocatalytically active color layer (thickness 140 μm) on a glass substrate optimized for the degradation of air pollutants.[44] The optical energy band gaps of Sto Photosan were estimated to be 3.01 eV. This difference might be caused by the thickness of the photoactive layers (140 μm), the particle sizes of the TiO_2, and potential additives in the color, which absorb in the range of visible light.

Pristine mesoporous TiO_2 film on a glass substrate shows activity that is 9% of theoretical photonic efficiency (Figure 7). With deposition on ITO-coated glass, the activity increases to 14% due to the better defined pore system. Both samples already show a considerably higher ability to convert NO than Sto Photosan (6% of theoretical photonic efficiency) probably due to the much larger surface area of the mesoporous films, despite the fact that the paint exhibits a considerably higher thickness.

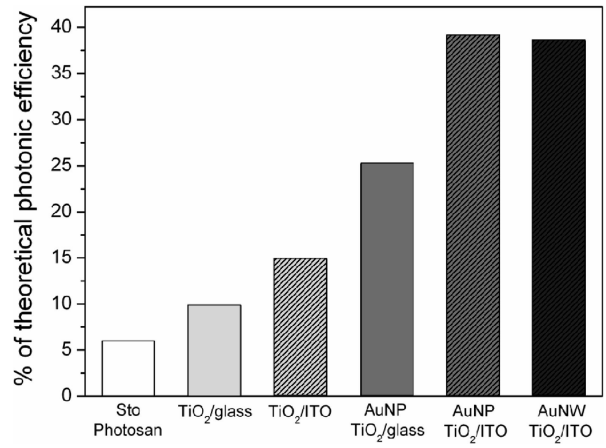

Figure 7. Comparison of photocatalytic activities of pristine and Au-loaded mesoporous TiO_2 films as well as commercial Sto Photosan Color.

Loading with Au nanoparticles smaller than 5 nm in size via the impregnation method leads to an increase in the activity by a factor of about 3, so that 26% of the theoretical value is reached for films on microscope glass slides and even 40% for films on ITO-coated glass (Figure 7, AuNP/TiO_2/glass or ITO). The major rate-limiting factor of photocatalytic activity is the fast recombination of photogenerated electrons and holes. Deposited gold nanoparticles provide a more efficient charge separation of the electron−hole pairs and an increase of their lifetime.[10,38,45,46] The gold nanoparticles are very effective traps for electrons due to formation of a Schottky barrier at the metal−semiconductor contact. A requirement, however, is that the Au nanoparticles are in close contact to crystalline TiO_2. If the anatase particles are linked together, this additionally leads to an enhanced transfer of electrons to the gold nanoparticles, resulting in a further increase in photonic efficiency.

Dendritic gold nanostructures electrodeposited in the pore system of the mesoporous TiO_2 film prepared on ITO-coated glass show 39% of the theoretical photonic efficiency (Figure 7, AuNW/TiO_2/ITO), almost the same value as that for gold nanoparticles incorporated by the impregnation method. This result indicates that the morphology of incorporated gold nanostructures seems to have almost no influence on photocatalytic efficiency. Consequently, pulsed electrodeposition appears as the preferable method for the incorporation of Au, since virtually the same enhancement in the photocatalytic efficiency can be achieved in a much simpler way.

Au nanostructures of the two most efficient samples, both with Au:Ti ratios about 0.08, have been compared in more detail by use of high-resolution transmission electron micrographs (Figure 8). Both images clearly reveal the presence of the necessary nanocontacts between noble metal nano-

(38) Kamat, P. V. *Chem. Rev.* **1993**, *93*, 267.
(39) Hoffman, M. R.; Martin, S. T.; Choi, W.; Bahnemann, D. W. *Chem. Rev.* **1995**, *95*, 69.
(40) Tutchi, A. S.; Ollis, D. F. *J. Catal.* **1990**, *122*, 178.
(41) Devahasdin, S.; Fan, C., Jr.; Li, K.; Chen, D. H. *J. Photochem. Photobiol., A* **2003**, *156*, 161.
(42) Wang, H.; Wu, Z.; Zhao, W.; Guan, B. *Chemosphere* **2007**, *66*, 185.
(43) Lim, T. H.; Jeong, S. M.; Kim, S. D.; Gyenis, J. *J. Photochem. Photobiol., A* **2000**, *134*, 209.
(44) http://www.sto.de.
(45) Sakthivel, S.; Shankar, M. V.; Palanichamy, M.; Arabindoo, B.; Bahnemann, D. W.; Murugesan, V. *Water Res.* **2004**, *38*, 3001.
(46) Arabatzis, I. M.; Stergiopoulos, T.; Andreeva, D.; Kitova, S.; Neophytides, S. G.; Falaras, P. *J. Catal.* **2003**, *220*, 127.

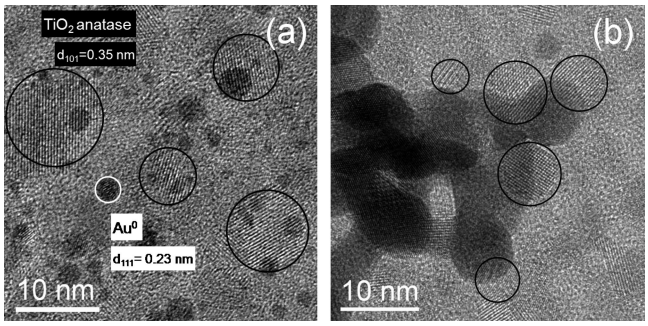

Figure 8. High-resolution TEM micrographs of Au-loaded mesoporous TiO_2 films with Au:Ti ratio of about 0.08, synthesized by (a) impregnation method and (b) pulsed electrodeposition.

particles and crystalline anatase phase. In both samples TiO_2 anatase nanocrystals 5−10 nm in size were observed. This result agrees well with the investigations by X-ray diffraction and Li insertion, which were reported previously[18,47] and reveal that the TiO_2 films, synthesized by Pluronic P 123, consist of a mixture of about 50 mass % anatase nanoparticles as photocatalytic active species, small amounts of TiO_2(B), and regions of amorphous TiO_2.

The mesoporous Au/TiO_2 film with Au loaded by the impregnation method exhibits spherical gold nanoparticles 2 nm in size, considerably smaller than the anatase nanocrystals (Figure 8a). On the other hand, the electrodeposited Au nanostructures 9 nm in width and up to 100 nm in length are larger than the anatase crystals. But this difference seems to have almost no influence on photocatalytic activity.

Figure 9a demonstrates the dependence of photocatalytic activity on Au:Ti ratio for films prepared by impregnation and reduction with $NaBH_4$. Films on ITO still show the same activity with Au:Ti ratio of 0.28 as they show with Au:Ti ratio of 0.08. When the Au:Ti ratio is increased to 0.54, however, both the films on ITO and those on glass exhibit clearly lower photocatalytic activities. A similar trend was reported for TiO_2 films loaded with Pt and ascribed to an increase in the particle size with increasing metal content.[48] If the dendritic Au structures get too long in the wormhole-like pore system, their accessibility for the reactants decreases and slight blocking effects hinder oxygen diffusion to the Au nanostructures and reactivity with the electrons stored on the Au. If the electron density on Au gets too high, the migration of photogenerated electrons from the TiO_2 framework is reduced and consequently electron−hole recombination on the TiO_2 nanocrystals becomes more prominent.

A further enhancement in the photonic activity up to almost 60% of the theoretical value can be achieved by pretreatment of the surface with O_2 plasma (Figure 9b). This treatment is a fast and simple method for the formation of superhydrophilic surfaces, which was previously reported by Boinovich and Emelyanenko.[49] Plasma etching leads to a considerable increase in the photonic efficiency due to the high amount of hydroxyl groups on the surface, which is

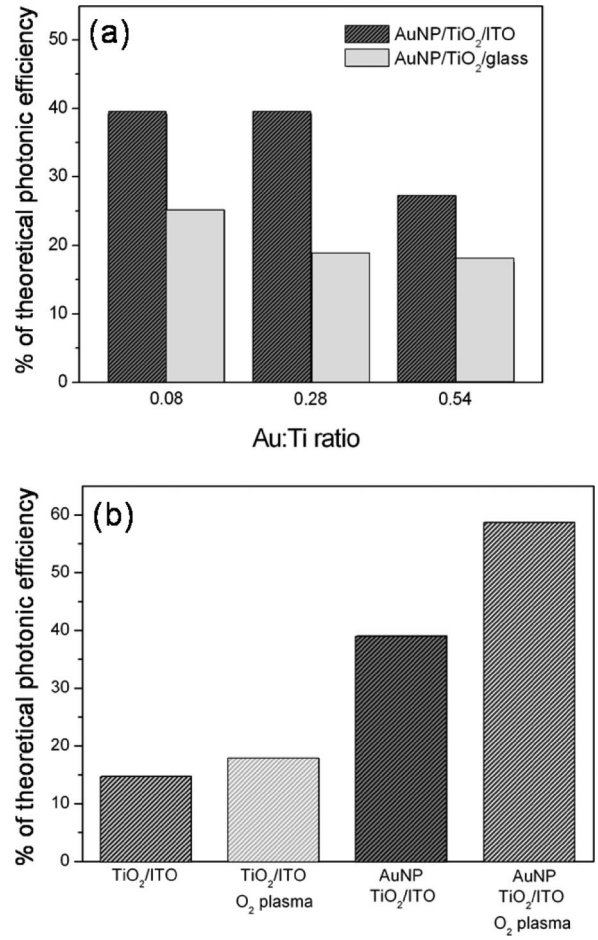

Figure 9. (a) Dependence of photonic efficiency of Au/TiO_2 nanocomposite films with Au loaded by impregnation on the Au:Ti ratio. (b) Enhancement of photocatalytic activity of TiO_2 films with and without Au by O_2 plasma treatment (Au:Ti ratio 0.08).

vitally important in the photocatalytic oxidation of NO. Measurement of the contact angle for water showed that while values of 8−15° were obtained for untreated films, treatment with O_2 plasma led to a drastic decrease to less than 3°, which corresponds to a superhydrophilic surface.

IV. Summary and Conclusions

Mesoporous Au/TiO_2 nanocomposites were synthesized by two methods: (i) impregnation followed by reduction of the metal precursor and (ii) pulsed cathodic electrodeposition. The former method leads to mesoporous TiO_2 films with red color caused by spherical gold nanoparticles smaller than 5 nm in size. By pulsed electrodeposition, dendritic Au nanostructures were exclusively generated inside the pores of the mesoporous TiO_2 films as a replica of the pore system, which results in films with a blue color caused by a red shift of the surface plasmon resonance. Variation of the number of pulses influences the density of the nanostructures in the ordered mesoporous TiO_2 template. If low-potential pulses are applied, exclusive growth of nanowires from the conductive ITO layer through the film results.

The character of the porous system depends on the surface properties of the support, being monomodal for amorphous glass sheets and bimodal for the conductive glass, whose surface is covered with an ITO layer. Incorporation of both

(47) Fattakhova-Rohlfing, D.; Wark, M.; Brezesinski, T.; Smarsly, B. M.; Rathousky, J. *Adv. Funct. Mater.* **2007**, *17*, 123.
(48) Bosc, F.; Ayral, A.; Keller, N.; Keller, V. *Appl. Catal., B* **2007**, *69*, 133.
(49) Boinovich, L. B.; Emelyanenko, A. M. *Russ. Chem. Rev.* **2008**, *77*, 583.

gold nanoparticles and dendritic nanostructres or nanowires fills some parts of the pore system but does not substantially change the characteristics of the remaining open mesopore system.

In the photocatalytic oxidation of NO, the presence of gold nanoparticles and dendritic nanostructures in the pores of TiO_2 films substantially increases the photocatalytic activity by a factor of about 2 or 3, from 9% up to 26% and about 40% of the theoretical photon efficiency depending on the applied porous system, which are considerably higher than the values found for commercially available reference materials (<10%). The activity can be further enhanced to almost 60% if superhydrophilic surfaces are formed by treatment with oxygen plasma. Because high Au:Ti ratios limit the photocatalytic activity due to some gas diffusion hindrance, resulting in higher electron−hole pair recombination rates, the best photocatalytic results were obtained with Au loadings of less than 20 mass % (Au:Ti ratio $\approx$ 0.08).

Acknowledgment. We thank Professor Dr. J. Caro (Institute of Physical Chemistry, Leibniz Universität Hannover) for fruitful discussions. Financial support by the German Science Foundation (DFG, WA 1116/12-1) in the frame of the priority program SPP 1165 "Nanowires and nanotubes" and by the Grant Agency of the Czech Republic (Project 104/08/0435) is gratefully acknowledged.

CM803455K